Step loading corrosion fatigue testing of 7075-T6 WC/C coated specimens in air and methanol

Sergio Baragetti[1,2,*], Riccardo Gerosa[3] and Francesco Villa[1]

[1] *Department of Engineering Management, Information and Production Engineering, University of Bergamo, Viale Marconi 5, Dalmine 24044, Italy*

[2] *GITT - Centre on Innovation Management and Technology Transfer, University of Bergamo, Via Salvecchio 19, Bergamo 24129, Italy*

[3] *Politecnico di Milano, Polo territoriale di Lecco, Via Gaetano Previati 1/c, 23900 Lecco, Italy*

[*]***corresponding author*** *– e-mail:* *sergio.baragetti@unibg.it*, *phone: +39 035 205 2382, address: Viale Marconi 5, Dalmine 24044, Italy*

Abstract

7075-T6 aluminum alloy, despite its high mechanical performances, has shown critical issues due to its sensitivity to corrosion. In the present work, a Tungsten Carbide / Carbon (WC/C) thin hard coating has been evaluated for its effects on corrosion fatigue behavior on a 7075-T6 substrate, by means of rotating bending (R = -1) step-loading tests at $2 \cdot 10^5$ cycles, in laboratory air and methanol, with different surface finishing. A corrosion fatigue protection effect was found for the smoothest specimens, along with detrimental fatigue effects caused by the high applied stresses and the coating process thermal effects. SEM analysis has been performed to characterize the fracture surfaces.

Keywords: 7075-T6, Aluminum alloys, Corrosion Fatigue, Methanol, Thin films, WC/C.

1. Introduction

In the recent decades, the worldwide rise in the energetic demand, and the increasing concern regarding the environmental aspects of the transportation industry have shifted the engineering design effort towards more efficient systems, in the aerospace, automotive and maritime application fields. In terms of structural design, an increase in efficiency means to increment the strength-to-mass ratio of the designed components, by adopting lightweight materials with brilliant mechanical characteristics. In the automotive sector, the adoption of aluminum light weight components is increasing, especially regarding high performance vehicles. The general trend, however, is to extend the adoption of these alloys in the mass production of motor vehicles, by designing lightweight cars for the most popular segments with a percentage of aluminum alloys superior to 50 % [1]. Concerning high performance *Al-Zn-Mg* 7000 series alloys, their usage is still scarce in the automotive mass production, mainly due to their difficult weldability and their sensitivity to the high temperatures involved in the stamping processes. The industrial and the research worlds are however striving to reach satisfactory solutions to both issues. Recent developments of the Friction Stir Welding (FSW) technique for lightweight alloys welding seem to encourage a wider adoption of these materials in the industrial manufacturing processes, in light of the positive results encountered for the 7000 series [2,3]. A sufficient knowledge on the effects of the FSW process parameters on the mechanical performances of the welded materials still has to be reached, since deep microstructural and mechanical modifications have been found by slight variations of welding rate, rotational speed and tool shape [4]. Concerning the adoption of high performance aluminum alloys in stamping processes, in the work by Kumar *et al.* [5] cross die and swift cupping formability tests have been performed on 7020-T6 AA, highlighting a suitable behavior of the alloy for automotive stamping at temperatures above 200 °C. The mechanical characteristics, evaluated by means of tensile tests obtained both from heated specimens and from specimen extracted from formed sheets, showed a decrease of approximately 30% in terms of UTS for the warm formed and paint baked 7020-T6 sheets. A minimum YS above 220 MPa was however found for 7020-T6 sheets after warm forming between 200 and 220 °C.

Nomenclature

ΔS [MPa]: stress increment between two consecutive load blocks	S [MPa]: fatigue strength
N: fatigue life number of cycles	S_N [MPa]: fatigue strength for a N cycles fatigue life
N_f: fatigue life number of cycles of the failed block	$S_{N=2\cdot10^5}$ [MPa] fatigue strength for a $2\cdot10^5$ cycles fatigue life
N_{conf}: fatigue life number of cycles of the confirmation run	S_{pf} [MPa]: fatigue load applied at the load block prior to failure
R: fatigue test load ratio $\sigma_{min}/\sigma_{max}$	S_f [MPa]: fatigue load applied at the failed load block
R_a [μm]: average surface roughness	UTS [MPa]: ultimate tensile strength
	YS [MPa]: yielding strength

In order to widen the application field of high strength-to-mass ratio aluminum light alloys to more demanding structural engineering applications, new strategies must be developed to overcome the critical aspects of this class of materials. 7075-T6 aluminum alloy is one of the most interesting materials for this purpose: it has been developed and widely employed in the aeronautic sector as one of the most performant materials in terms of strength-to-mass ratio. However, some critical aspects linked to this high performance alloy prevent its further usage in the mechanical design of components.

The main weak spot of 7075 AA in the T6 temper is linked to its corrosion behavior. Several literature sources have highlighted its susceptibility to pitting, crevice, intergranular and exfoliation corrosion [6-8]. Environments which presents NaCl-water mixtures have proven to be particularly detrimental in terms of 7075 Stress Corrosion Cracking (SCC) behavior in the T6 temper [9]. In order to reduce the effects of SCC on commercial applications of the 7075 alloy, the 7x class of aging treatments has been introduced to obtain corrosion resistance, the use of 7075-T6 being interdicted for recent aeronautical designs [7]. The improved SCC resistance of the 7075-T7x alloys comes however at the price of a non-negligible reduction of mechanical performances [7,8,10]. Efforts to find an acceptable compromise between a satisfying corrosion behavior and a limited drop in UTS and YS by means of appropriate ageing processes, have been carried on in [7,8]. The results are encouraging, especially for intergranular corrosion [8], but a certain reduction in the mechanical properties is still to be expected [7].

Concerning fatigue loads, it is well known that the 7075-T6 fatigue strength decreases dramatically in a NaCl-water environment from pitting corrosion, both from salt spray fog exposure [11] and from continuous immersion during fatigue tests [12,13]. In [12], a reduction of a factor 2.9 in terms of fatigue strength at high cycles is found, and the author highlights that the effects of corrosion during dynamic loads application is much more severe than the effects of pre-corroded specimens. In [13], rotating bending fatigue tests in NaCl 3.5 wt. % solution are performed at higher applied stresses, showing a significant fatigue strength decrease of about 20% at $1\cdot10^5$ cycles.

As an alternative to metallurgical processes, several efforts have been made in literature with the aim to improve the 7075-T6 corrosion fatigue performances, to restore the application field of the alloy and to extend its usage in new design solutions, by means of protective coatings [12-14]. Its brilliant mechanical characteristics are in fact extremely desired for the design of lightweight structural components subject to static and fatigue loading. Genel [12] tested oxide coated 7075-T6 rotating bending fatigue specimens. The 23 μm thick coating, realized by means of sulfuric acid anodizing process, produced a remarkable reduction in terms of fatigue strength in laboratory air. The corrosive testing in 3.5 wt. % NaCl-water solution revealed that pit formation was increased by the combined action of corrosion and fatigue loads. The coated specimens showed superior behavior during static corrosion tests, but their performance during corrosion fatigue tests depended on the applied stresses: at high applied stresses, the coated specimens exhibited a worse fatigue strength with respect to the uncoated ones, while better performances were achieved at lower applied stresses, *i.e.* higher number of cycles in the S-N diagram, the turning point of this behavior being around $1\cdot10^5 \div 1\cdot10^6$ cycles. The fatigue performances of the coated alloy showed slight changes between air and corrosive environment, suggesting that a significant reduction in terms of fatigue strength was caused by the coating procedure. The fatigue strength of coated the specimens never reached those of bare samples in air, regardless of the number of cycles N.

A significant portion of the research work on corrosion fatigue protection by means of functional coating has focused on the field of Physical Vapor Deposition (PVD) processes for the generation of thin hard coatings [13-16]. PVD coatings are increasingly used in industrial manufacturing processes, due to their capability to increase the surface characteristics of metallic materials, in terms of hardness increase, corrosion and wear resistance, by means of more controlled and less polluting deposition techniques, with respect to industrial electroplating and electrochemical processes [17,18]. Several experimental works have explored the contribution of PVD coatings in terms of fatigue behavior.

The application of thin hard coatings on steel substrates usually leads to beneficial contributions in terms of fatigue strength [19,20]. In the work by Baragetti *et al.*[19], Chromium Nitride (CrN) deposition on H11 tool

steel and 2205 duplex stainless steel produced beneficial effects at different fatigue lives, both in the high and low cycle regimes. Corresponding results have been found in the experiments of Puchi-Cabrera *et al.* [20], for a Titanium Nitride (TiN) coating on AISI 316L stainless steel. These positive results are often linked to the high compressive residual stresses introduced in the substrate by the coating deposition process, which typically prevent crack nucleation and propagation [16,21-24]. A detailed analysis of the contribution of residual stresses to the improvement of fatigue life, from the point of view of fracture mechanics, has been pointed out by means of FE analysis in [22,23].

Another significant trend regarding fatigue corrosion behavior, as found in various experimental works on PVD coated steels [21,25], consists in a positive fatigue contribution of the thin hard coating at fatigue lives superior to $1 \cdot 10^5$ cycles, while for inferior lives and higher applied stresses, the coating shows a detrimental effect on the fatigue strength of the coated steel substrates. Saini and Gupta [21] found exactly such a behavior for a 2 μm thick Tungsten Carbide / Carbon (WC/C) coating deposited over a SAE8620 case carburized steel substrate, by means of rotating bending ($R = -1$) fatigue tests. The authors justify such trend by noticing that, for high applied stresses regions, the high deflection of the substrate surface cause multiple cracking in the thin hard coating, some of which can propagate in the substrate. The same behavior of thin hard coatings, with cross-over with the uncoated material fatigue strength at $1 \cdot 10^5$ cycles, was found also by Su *et al.* in [25] for different Titanium and Chromium based PVD thin hard coatings such as TiN, Titanium Carbonitride – Ti(C,N), CrN, Chromium Carbonitride – Cr(C,N) on AISI 1035 steel, although in this case the authors do not assess the causes of such fatigue trends in the S-N curves. A schematic representation of the two behaviors found for PVD coatings on steel substrates is presented in Figure 1, inspired by the trends in the *S-N* fatigue curves reported in [19-21,25].
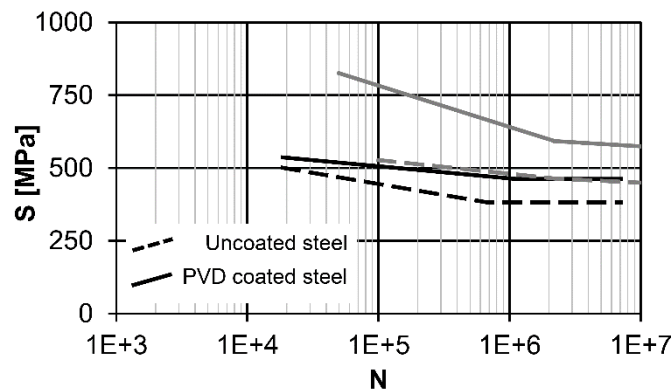
(a) Non-crossing behavior [19,20]
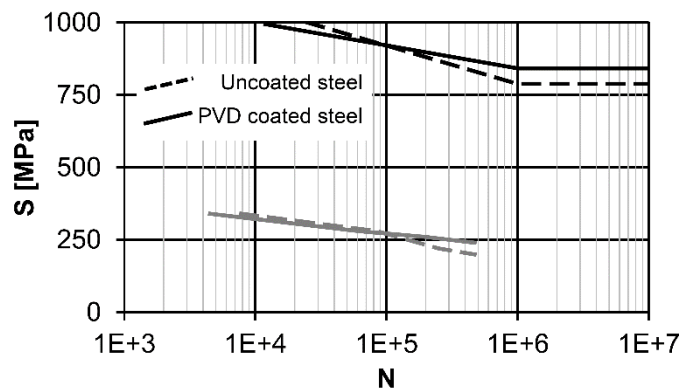
(b) Cross-over behavior [21,25]

Fig. 1 Typical behavior of PVD coated steel substrates: (a) non-crossing positive contribution of the coating [19,20]; (b) cross-over at $1 \cdot 10^5$ cycles, with beneficial contribution of the PVD coating at higher fatigue lives caused by residual stresses and detrimental contribution for lower fatigue lives due to excessive coating deformations at high applied stresses [21,25].

When considering the adoption of PVD coatings on light alloys, some further considerations must be taken into account. PVD coatings are much more critical on titanium and especially on aluminum substrates, and in

fact negative contributions in terms of fatigue strength have been highlighted in previous research work. In [24], rotating bending fatigue testing (R = -1) on Ti-6Al-4V Solution treated and overaged (STOA) titanium alloy, coated with a 3.9 µm TiN PVD layer, showed detrimental fatigue contribution of the coating between $1 \cdot 10^4$ and $1 \cdot 10^5$ cycles, for notched and smooth specimens. The authors underline that the coating can crack prematurely when critical strain is reached, or in presence of micro-defects, due to the brittle nature of the deposited layer.

As previously said, several PVD coatings have been proposed on a 7075-T6 aluminum substrate, to obtain corrosion fatigue protection [13,15] as well as other beneficial surface effects. In [13], rotating bending (R = -1) fatigue testing of uncoated and Zirconium Nitride (ZrN), 3 µm thick, coated 7075-T6 specimens has been performed, in laboratory air and in 3.5 wt. % NaCl-water mixture. The results highlight a significant, almost constant drop of 50÷70 MPa in terms of fatigue strength in the $1 \cdot 10^4 \div 1 \cdot 10^6$ fatigue life range, between the uncoated and the coated specimens in air. This results, obtained in contrast with the highly compressive residual stress pattern detected by the authors, discloses further mechanisms acting in the fatigue behavior of PVD coatings on 7075-T6 light aluminum alloys. The authors notice that two main mechanisms are responsible of this loss of fatigue strength. The first contribution is the reduction of the mechanical properties caused by the thermal loads of a ZrN PVD coating process, typically above 400 °C [13,26], which disrupts the mechanical characteristics granted by the T6 temper, which has an aging temperature of 121 °C [10,13,15]. The second detrimental mechanism is the coating cracking and delamination, which has been also detected on steel substrates at high applied stresses [21]. Results in the corrosive environment from [13] highlight however a certain potential protection from corrosion granted by the ZrN coating: when the fatigue life goes above $1 \cdot 10^5$, the fatigue strength of coated specimens in 3.5 wt. % NaCl approaches the strength of the uncoated specimens, suggesting that the delamination and cracking of the coating is reduced for lower applied stresses.

For which concerns the thermal degradation of the mechanical characteristics of the T6 temper on a 7075-T6 alloy, another significant work has been carried on by Oskouei and Ibrahim [15]. In the study, axial fatigue testing at R = 0.1 has been carried out on 7075-T6 flat specimens, uncoated and coated with a 3 µm TiN layer. A fatigue strength drop of more than 100 MPa has been found between $1 \cdot 10^5$ and $1 \cdot 10^6$ fatigue lives, according to the authors of [15] the reason is due to the high deposition temperatures of the PVD TiN coating, which are around 450 °C [15,26]. A post heat treatment is designed to recover the 7075-T6 fatigue characteristics after the TiN treatment, with acceptable results at least for short fatigue lives, while for N above $1 \cdot 10^5$ a certain reduction of the 7075-T6 mechanical properties is still found.

In the present work, extension of the proceedings presented in [27], the effects of a low temperature WC/C coating on the fatigue and the corrosion fatigue strength of a 7075-T6 aluminum alloy at a fatigue life of $2 \cdot 10^5$ cycles have been investigated, by means of a preliminary step-loading test campaign involving rotating bending (R = -1) tests in laboratory air and aggressive environment. The key idea beneath the present work is to protect the 7075-T6 alloy with a corrosion resistant thin hard coating with low deposition temperatures, in order to minimize the loss of mechanical properties of the substrate. Corroborated by rotating bending fatigue testing from a previous work [28] on 7075-T6 WC/C and DLC PVD coated and uncoated specimens, as well as on specimens which simulated the PVD processes thermal loads, a WC/C protective layer has been selected as the candidate for corrosion fatigue protection, expecting that its low deposition temperature of 180 °C [26,28], even if superior to the T6 ageing temperature of 121 °C [10], could prevent excessive losses in terms of fatigue strength. Two different surface finishing of the substrate were considered prior to deposition, in order to assess their effect on the fatigue and corrosion fatigue performances of both coated and uncoated specimens.

2. Materials and methods

Hourglass specimens have been lathe machined from commercial 7072-T6 bars, according to the ISO 1143 international standard [29], by the geometry reported in Figure 2. The base material chemical composition is reported in Table 1. The mechanical characteristics of the base material have been determined by means of tensile tests, performed by using an Instron 4507 machine, resulting in a UTS of 650 ± 1 MPa and a YS of 598 ± 1 MPa, from two samples. The material hardness was measured as 190 ± 2 HV, being obtained from three indentations using a Wolpert durometer.

Table 1. Chemical composition of the tested 7075-T6 aluminum alloy

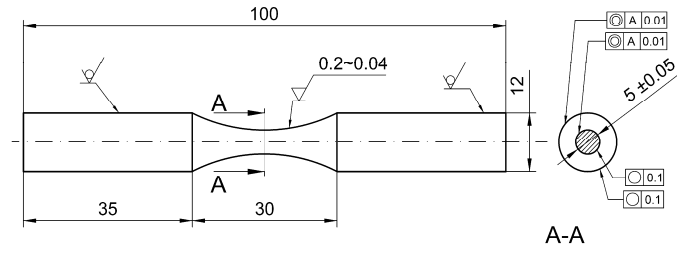| Al [%]	Zn [%]	Mg [%]	Cu [%]	Fe [%]	Si [%]	Cr [%]	Mn [%]	Ti [%]
Bal.	5,6	2,55	1,75	0,32	0,25	0,22	0,2	0,12

Fig. 2 Hourglass rotating bending fatigue geometry, according to the ISO 1143 standard [29].

The test area section of the machined specimens has been finished by following two different procedures, in order to create two sets of specimens with different average roughness R_a values. One set has been chosen to represent a rough, industrial grade surface finishing, the maximum R_a acceptable for industrial coatings being 0.2 µm [13,26]. The second set has been diamond polished to reach a mirror-like surface, minimizing the roughness effect on fatigue. To reach such effect, the first set of specimens was lathe finished with abrasive paper and lubricant from 600 to 1200 grit, creating circumferential grooves of the test section. The latter set has received further finishing in the longitudinal direction with a 1200 grit abrasive paper, then mirror-like polishing with 3 µm diamond paste in the longitudinal direction, according to the technical specifications of the coating facility [26]. Specimen test area was then cleaned with acetone to remove any trace of dust and diamond powder. Surface average roughness R_a was measured by means of a Form Talysurf profilometer, resulting in 0.29 µm for the rough finishing specimens and 0.04 µm for the as polished specimens, a value similar to other works on coated 7075-T6 rotating bending fatigue [13].

After the surface preparation, half of the two specimen sets were sent to industrial WC/C coating deposition at Lafer S.p.A. [26] (Piacenza, Italy) by means of PVD ion sputtering technique. Three layers were deposited in the commercial process, a first Cr sputtering layer, followed by a $WC+C_2H_2$ support layer and a $WC+C_2H_2$ functional layer. The overall coating thickness, as measured by SEM microscopy after coated specimen failure, was of about 2 µm. Two coated sets of rough and as polished fatigue specimens were obtained in this way.

Testing was conducted both in laboratory air and in continuous immersion in an aggressive, reagent grade ($\geq$ 99.8 wt. %) methanol environment. Methanol was chosen as the aggressive reference environment following experimental evidence of critical failures encountered in high performance lightweight alloys. Dramatic SCC and corrosion fatigue effects have been found after failures of Ti-6Al-4V pressurized tanks from the Apollo mission, filled by pure methanol as reference corroding environment [30,31]. Methanol and methanol water mixtures have been also used in recent axial corrosion fatigue step-loading testing of notched Ti-6Al-4V flat dogbone specimens, showing a highly detrimental contribution of this particular aggressive environment [32, 33].

To determine the fatigue strength at $2 \cdot 10^5$ cycles, the step-loading fatigue testing procedure has been followed. The procedure has been described in the ASTM Fatigue and Fracture Mechanics handbook series [34], as well as in an experimental campaign over titanium light alloys by Nicholas [35], and it has been validated for such lightweight alloys by Bellows *et al.* [36], where it is recommended also for fatigue testing of specimens whose fatigue performances are highly dependent from the single sample finishing or treatment, such as in our case. As anticipated previously, step-loading testing has been successfully adopted for corrosion fatigue tests of Ti-6Al-4V notched specimens [32,33].

The step loading method, as described in [34,35], consist in the testing of a single specimen for a single block of load cycles N, corresponding to the fatigue life limit of interest. If the specimen runs out, the load is raised of a value ΔS and the load block is repeated. The procedure is carried on until the specimen fails, at a number of cycles $N_f < N$. The fatigue strength S_N corresponding to the fatigue life N is then calculated by linear interpolation between the stress level of the last not failed block S_{pf} and the stress level of the failed block S_f, according to the formula:

$$S_N = S_{pf} + N_f / N \left(S_f - S_{pf} \right) \tag{1}$$

After the completion of the step loading procedure, a confirmation specimen is run at the identified fatigue strength S_N, to verify that the number of cycles obtained is consistent with the applied stress level. In the

present work, the step-loading fatigue tests, as well as the confirmation runs, have been performed by using an ItalSigma X2 TM 412 digital force control four point rotating bending machine, which allowed to control the applied stress with a resolution inferior to 1 MPa, for the specimen shape given in Figure 2.

3. Results and discussion

3.1. Step loading rotating bending fatigue tests

The results of the step loading procedure are reported in Figure 3, in terms of fatigue strength at $N = 2 \cdot 10^5$ cycles. The surface roughness influences as expected the fatigue behavior of the uncoated specimens in air, resulting in a 13% reduction in terms of fatigue strength. The uncoated specimens immersed in methanol exhibit a significant decrease of the fatigue strength, similar in magnitude to the drop experimented in [13] for 7075-T6 specimens dunked in 3.5 wt. % NaCl mixture. The methanol environment tends to level the fatigue strength of the specimens below the value of 200 MPa, regardless of the surface finishing, resulting in a reduction of -16% for the rough specimens, and of -29% for the mirror-like polished samples, with respect to laboratory air. This phenomenon could be perhaps owed to the fact that the aggressive environment disrupts the brilliant surface characteristics of the as-polished specimens, which in turn are not so excellent in the 1200 grit finishing.
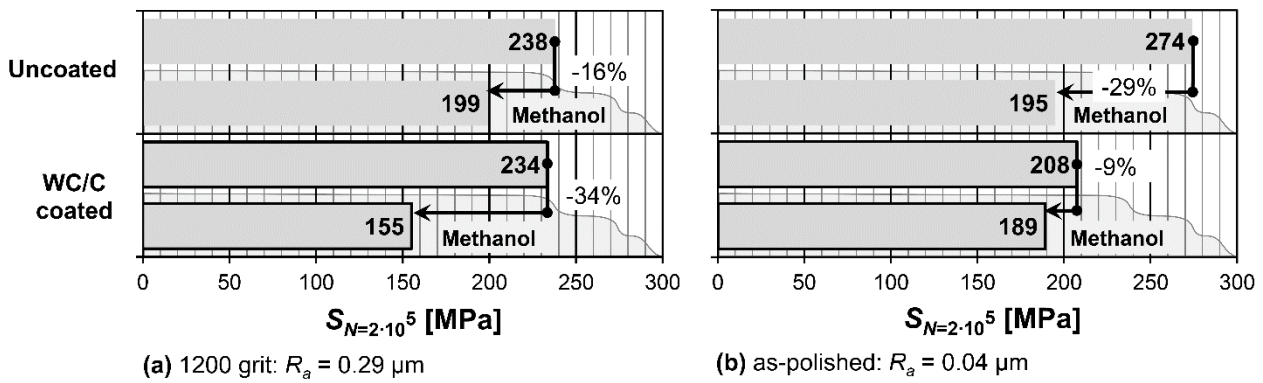

Fig. 3 Rotating bending step loading fatigue tests results in terms of fatigue strength for N = 2·10⁵ cycles on 7075-T6 uncoated and WC/C coated specimens, in laboratory air and in reagent grade methanol environment: (a) fatigue strength limits for rough surface preparation with 1200 grit paper; (b) fatigue strength limits for mirror-like polished specimens.

The coating process introduces a significant detrimental contribution, equal to a -24% fatigue strength drop between the coated and uncoated polished specimens, in agreement with the results found for other coatings [13,15]. In contrast with the substrate modifications found in [13,15], in the present case only a fraction of this drop can be attributed to the thermal loads, due to the low temperature PVD process, according to [28], where only a -6% drop has been found on 7075-T6 aluminum alloy due to thermal loads typical of WC/C PVD coatings, for 2·10⁵ cycles. The remainder component is attributable to the high deflections and shear stresses causing premature cracking and delamination of the coating at high applied stresses, following the mechanisms proposed in [13,21].

This consideration is corroborated by the fact that the higher roughness surface, generated by 1200 grit paper finishing, shows a drop of less than 2% in terms of fatigue strength, highlighting a lack of mechanical interaction between the substrate and the surface, caused by the poor coating adhesion.

If considering the coated specimens immersed in methanol, it can be immediately deduced from Figure 3 that a significant corrosion effect is found on the specimens with a mirror-like finishing, prior to WC/C deposition. The fatigue strength reduction is in fact of -9% with respect to laboratory air, if compared to a -34% detrimental effect found on roughly finished specimens, where corrosion protection was not achieved. This behavior underlines the lack of adhesion of the WC/C coating to surfaces finished at the rough extreme of the industrial standards [13,26], highlighting the 1200 grit paper, $R_a = 0.29$ µm preparation of the surfaces as unsuitable for the corrosion protection behavior. A surface finishing smoother than the actual standards is recommended, i.e. $R_a < 0.1$ µm, according to the present work and to [13].

In order to confirm the results obtained by the step loading procedure, and presented in Figure 3, some confirmation runs have been performed at the stress levels identified in Figure 2, and are presented in Table 2.

Table 2. Confirmation run failure number of cycles N_{conf} obtained for the $2 \cdot 10^5$ fatigue strengths for different samples

Specimens	Environment	$S_{N = 2 \cdot 10^5}$ [MPa]	N_{conf}
Uncoated, as polished	Air	274	$1.2 \cdot 10^5$
Uncoated, as polished	Methanol	195	$2.5 \cdot 10^6$
Uncoated, 1200 grit paper	Air	238	$4.5 \cdot 10^5$
WC/C coated, 1200 grit paper	Air	234	$3.0 \cdot 10^5$
WC/C coated, as polished	Methanol	189	$1.2 \cdot 10^6$

The confirmation runs show a dispersion of N_{conf} at the tested load levels which is compatible with other fatigue results for 7075-T6 specimens [13], considering both the uncoated and the coated specimens in air. For the corrosion fatigue testing in methanol, the confirmation runs showed higher N_{conf} values, suggesting that the corrosion fatigue is more aggressive by adopting a step-loading procedure. This phenomenon is probably caused by the immersion times, which are necessary limited for a single confirmation run, although further experimental testing must be carried on to investigate this aspect. The results obtained in Figure 3 are hence to be considered conservative for which regards testing in methanol, thus corroborating the protective role of the WC/C coating on the 7075-T6 as-polished substrate.

3.2. SEM observations of the fracture surface

The fracture surfaces have been observed by SEM. In Figures 4 and 5 a comparison is reported among the WC/C coated specimens tested respectively in laboratory air and methanol solution, varying the surface finishing.
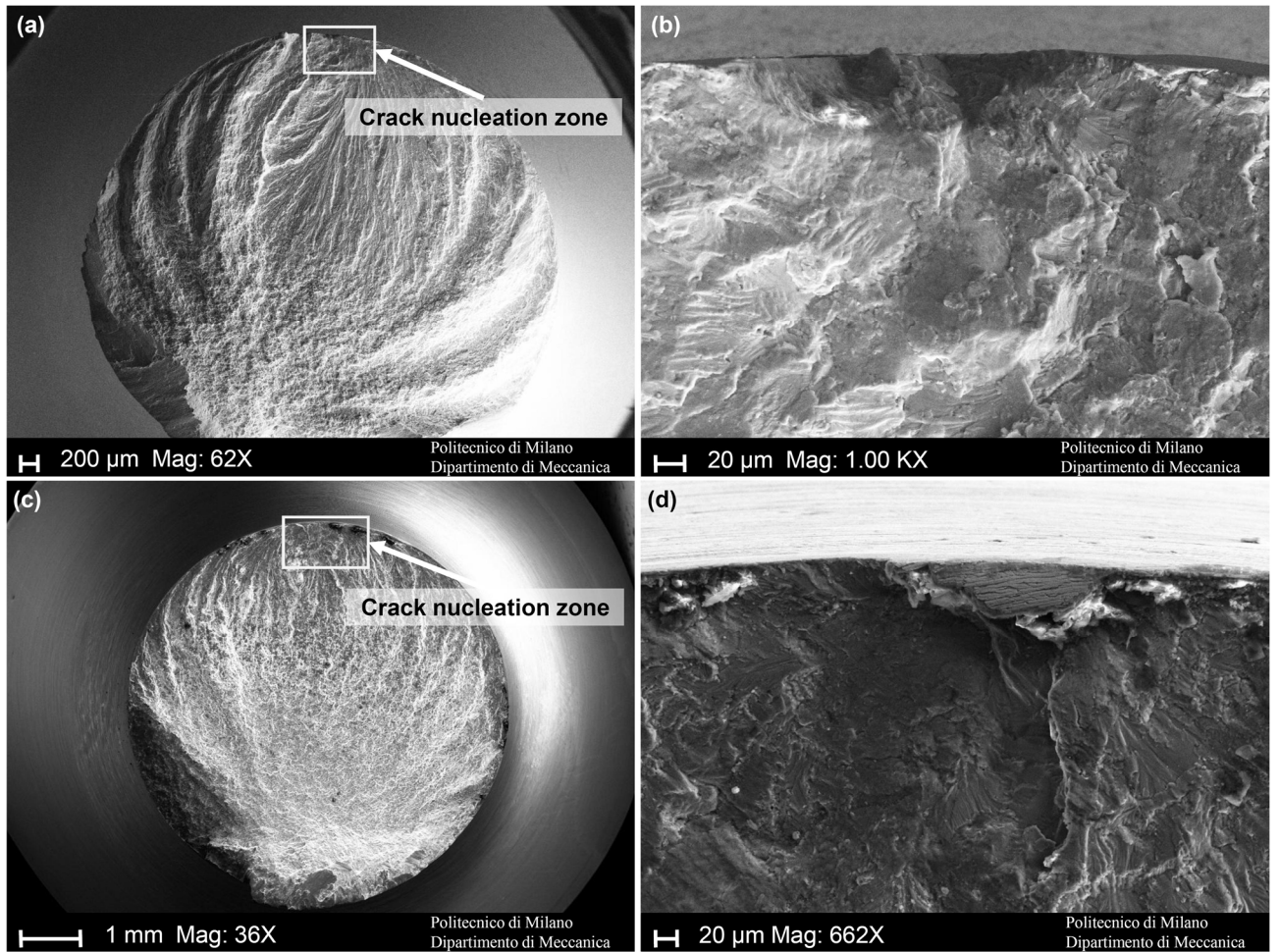

Fig. 4 WC/C coated specimens tested in air with different finishing: pictures (a) and (b) refer to the diamond polished sample tested at 208 MPa – (b) is a magnification of (a) in the crack nucleation zone; pictures (c) and (d) refer to the 1200 grit paper polished sample tested at 234 MPa – (d) is a magnification of (c) in the crack nucleation zone.
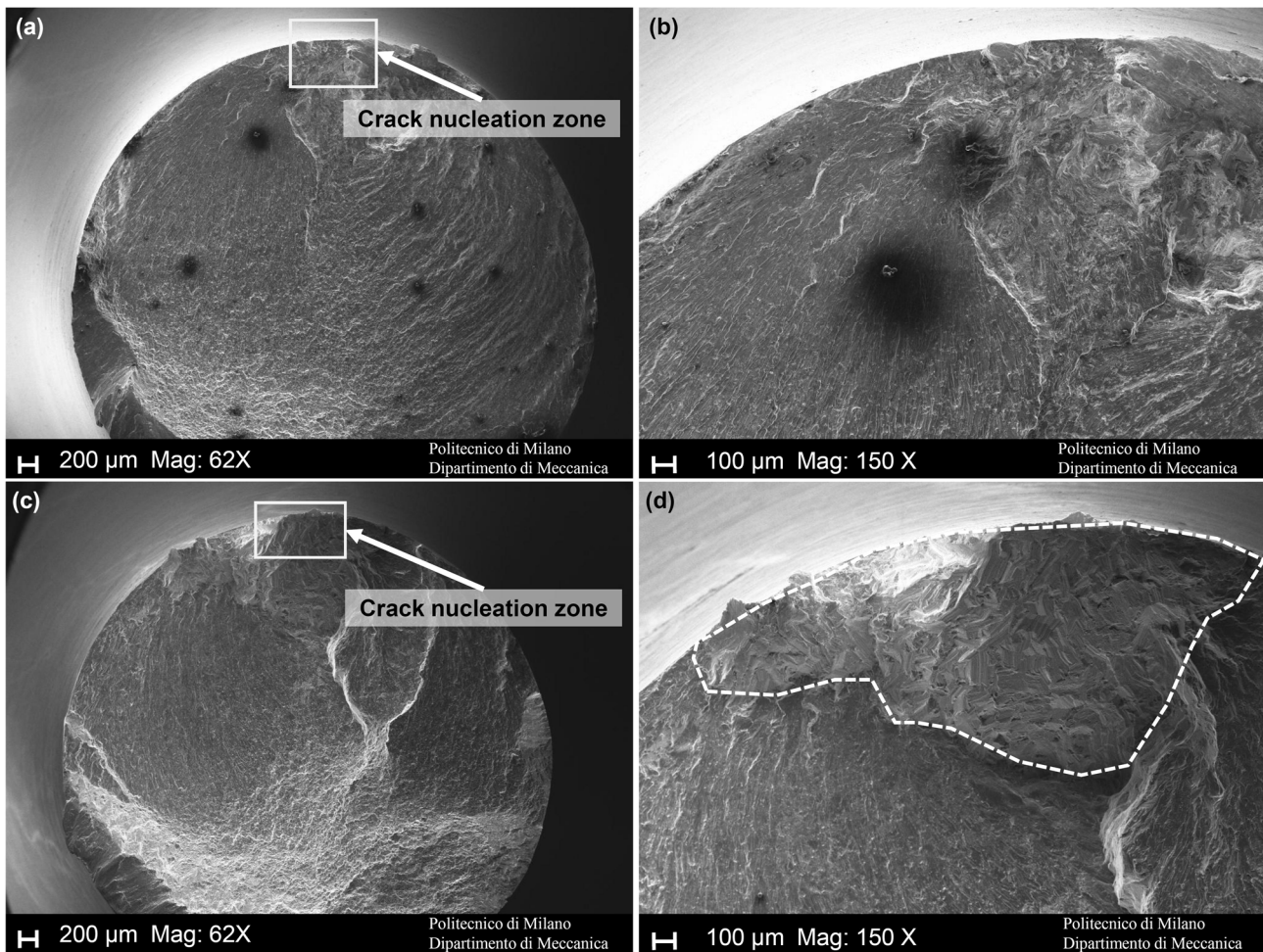
Fig 5 WC/C coated specimens tested in methanol solution with different finishing: pictures (a) and (b) refer to diamond polished sample tested at 189 MPa – (b) is a magnification of (a) in the crack nucleation zone; pictures (c) and (d) refer to 1200 grit paper polished sample tested at 155 MPa – (d) is a magnification of (c) in the crack nucleation zone.

In the coated specimens, the crack seems to nucleate at the metal/coating interface. Nevertheless, the lower fatigue limit of the diamond polished samples tested in air can be related to a premature cracking of the coating that propagates inside the substrate. As previously said, this is a known phenomenon especially when loads are high [13,21]. In the 1200 grit paper polished samples, instead, the weaker adhesion of the coating on the substrate could prevent such a mechanism.

As seen in section 3.1, the diamond polished samples tested in the methanol solution resulted in a better fatigue behavior with respect to the corrosion fatigue of 1200 grit paper prepared specimens. Even if a good adhesion of the coating on the diamond polished substrate can result in an anticipated cracking, the presence of an adherent coating protects the substrate from the aggressive environment. A weaker bond among the coating and the substrate can instead result in an anticipated contact between the metal and the methanol solution. The fracture surfaces shown in Figure 5, in fact, show that the 1200 grit paper polished sample shows a pretty wide zone damaged by the methanol solution. The same kind of damage can be observed in Figure 6 that refers to an uncoated diamond polished sample tested in methanol solution.
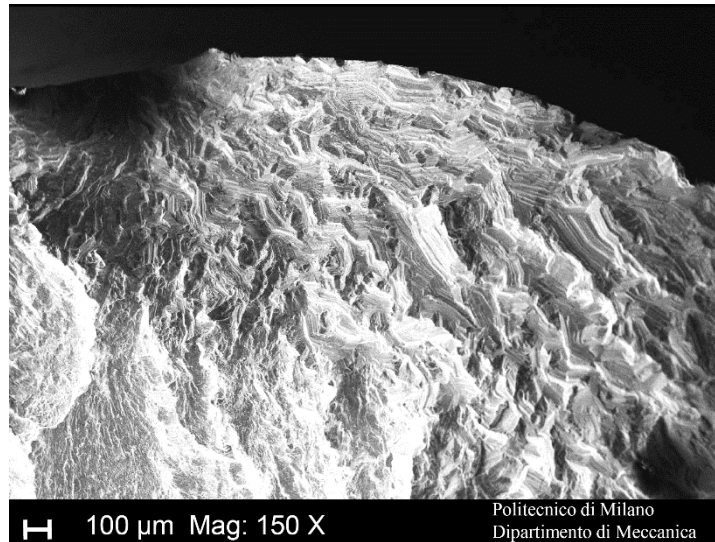
Figure 6. Uncoated diamond polished specimen tested in methanol solution at 195 MPa.

4. Conclusions

In the present work, corrosion fatigue behavior of WC/C coated and uncoated 7075-T6 aluminum alloy specimens has been investigated, by means of rotating bending ($R = -1$) fatigue tests. The samples were tested in laboratory air and in a reagent grade (≥ 99.8 wt. %) methanol environment, to determine their fatigue strength for an expected life of $2 \cdot 10^5$ cycles. The step-loading procedure was adopted, by testing samples over $N = 2 \cdot 10^5$ blocks at increasing applied loads, followed by confirmation runs at the fatigue strength found.

Two different substrate finishing in the test area were considered: a 1200 grit abrasive paper finishing, with $R_a = 0.29$ µm representing the coarser industrial finishing allowed for PVD coating, and a mirror-like diamond polished surface, with $R_a = 0.04$ µm.

SEM observation of the fracture surface of the samples were performed both on coated and uncoated failed specimens, for the different tested surface finishing and environmental combinations, to individuate the nucleation zones and the effects of the coatings and of the aggressive methanol corrosive medium.

The experimental activity highlighted the following evidences:

- The methanol environment resulted to be highly detrimental for the uncoated 7075-T6 alloy corrosion fatigue behavior, by reducing the fatigue strength at $2 \cdot 10^5$ cycles below 200 MPa, regardless of the surface finishing.
- The mechanical effect of the WC/C coating on the 7075-T6 substrate was profoundly affected by the substrate roughness. In particular, mirror-like polished specimens experienced a detrimental effect from the WC/C coating in air, *i.e.* -24% in terms of fatigue strength, due to the interaction between the thin hard coating and the substrate at high applied stresses, where premature cracking of the coating is expected. For the same reason, specimens prepared with 1200 grit paper showed no significant reduction of the fatigue strength (-6%), since the WC/C coating was not able to interact mechanically with the substrate due to poor adhesion.
- For the same reasons, the WC/C coating on the smooth specimens has resulted in an enhanced corrosion protection (-9% of fatigue strength drop) if compared to the 1200 grit paper prepared samples, whose scarce adhesion to the aluminum substrate resulted in a -34% performance on fatigue strength. Rougher surface preparations are hence not recommended for the use of a WC/C PVD layer for corrosion protection at high applied stresses, an average roughness $R_a < 0.1$ µm being more suitable for this purpose.
- SEM observation of the fracture surfaces allowed the identification of the nucleation and propagation zones. Moreover some details of the fracture surface seems to be in good agreement with the fatigue limits determined in the experimental tests, especially the ones performed in the aggressive environment, corroborating the idea that a good 7075-T6 corrosion protection is achieved by WC/C coating on mirror-like finished substrates.

5. Acknowledgments

6. Funding

7. References

[1] J. Hirsch. Aluminium in Innovative Light-Weight Car Design, Materials Transactions 52(5): 818-24, 2011.

[2] S. Lomolino, R. Tovo, J. dos Santos. On the fatigue behaviour and design curves of friction stir butt-welded Al alloys. Int. J. Fatigue 27: 305-16, 2005.

[3] P. Cavaliere, R. Nobile, F. W. Panella, A. Squillace. Mechanical and microstructural behaviour of 2024–7075 aluminium alloy sheets joined by friction stir welding. Int. J. Mach. Tool. Manu. 46: 588-94, 2006.

[4] S. Baragetti, G. D'Urso. Aluminum 6060-T6 friction stir welded butt joints: fatigue resistance with different tools and feed rates. J. Mech. Sci. Technol. 28(3): 867-77, 2013.

[5] M. Kumar, N. Sotirov, C.M. Chimani. Investigations on warm forming of AW-7020-T6 alloy sheet. J. Mater. Process. Tech. 214: 1769-76, 2014.

[6] A. El-Amoush. Intergranular corrosion behavior of the 7075-T6 aluminum alloy under different annealing conditions. Mater. Chem. Phys. 126: 607-13, 2011.

[7] G. Silva, B. Rivolta, R. Gerosa, U. Derudi. Study of the SCC Behavior of 7075 Aluminum Alloy After One-Step Aging at 163 °C. J. Mater. Eng. Perform. 22(1): 210-4, 2013.

[8] J. Li, Z. Peng, C. Li, Z. Jia, W. Chen, Z. Zheng, Mechanical properties, corrosion behaviors and microstructures of 7075 aluminium alloy with various aging treatment. Trans. Nonferrous Met. Soc. China 18: 755-62, 2008.

[9] M. Hyatt, M. Spidel. High strength aluminum alloys, in Stress Corrosion Cracking in High Strength Steels and in Titanium and Aluminum Alloys. Ed. Brown, BF, Washington D.C., Naval Research Lab, pp. 174-7, 1972.

[10] Matweb website, www.matweb.com, 2014.

[11] K. K. Sankaran, R. Perez, K. V. Jata. Effects of pitting corrosion on the fatigue behavior of aluminum alloy 7075-T6: modeling and experimental studies. Mater. Sci. Eng. A297:223–9, 2001.

[12] K. Genel. Environmental effect on the fatigue performance of bare and oxide coated 7075-T6 alloy. Eng. Fail. Anal. 32: 248-60, 2013.

[13] E. S. Puchi-Cabrera, M. H. Staia, E. A. Ochoa-Pérez, D. G. Teer, Y. Y. Santana-Méndez, J. G. La Barbera-Sosa, D. Chicot, J. Lesage. Fatigue behavior of AA7075-T6 aluminum alloy coated with ZrN by PVD. Int. J. Fatigue 30: 1220-30, 2008.

[14] C. Charrier, P. Jacquot, E. Denisse, M. J. P. Millet, H. Mazille. Aluminium and Ti/Al multilayer PVD coatings for enhanced corrosion resistance. Surf. Coat. Technol. 90: 29-34, 1997.

[15] R. H. Oskouei, R. N. Ibrahim. The effect of a heat treatment on improving the fatigue properties of aluminium alloy 7075-T6 coated with TiN by PVD. Procedia Eng. 10: 1936-42, 2011.

[16] L. Cunha, M. Andritschky, Residual stress, surface defects and corrosion resistance of CrN hard coatings. Surf. Coat. Technol. 111: 158-62, 1999.

[17] R. Gåhlin, M. Larsson, P. Hedenqvist. ME-C:H coatings in motor vehicles. Wear 249: 302-9, 2001.

[18] B. Navinšek, P. Panjan, I. Milošev. PVD coatings as an environmentally clean alternative to electroplating and electroless processes. Surf. Coat. Technol. 116-119: 476-87, 1999.

[19] S. Baragetti, M. Gelfi, G. M. La Vecchia, N. Lecis. Fatigue resistance of CrN thin films deposited by arc evaporation process on H11 tool steel and 2205 duplex stainless steel. Fatigue Fract. Eng. Mater. Struct. 28(7): 615-21, 2005.

[20] E. S. Puchi-Cabrera, F. Matínez, I. Herrera, J. A. Berríos, S. Dixit, D. Bhat. On the fatigue behavior of an AISI 316L stainless steel coated with a PVD TiN deposit. Surf. Coat. Technol. 182: 276-86, 2004.

[21] B. S. Saini,V. K. Gupta. Effect of WC/C PVD coating on fatigue behaviour of case carburized SAE8620 steel. Surf. Coat. Technol. 205: 511-18, 2010.

[22] S. Baragetti. Fatigue resistance of steel and titanium PVD coated spur gears. Int. J. Fatigue 29, p. 1893–903, 2007.

[23] S. Baragetti, G. M. La Vecchia, A. Terranova. Variables affecting the fatigue resistance of PVD-coated components. Int. J. Fatigue 27: 1541-50, 2005.

[24] S. Baragetti, L. Lusvarghi, F. Pighetti Mantini, F. Tordini. Fatigue Behaviour of Notched PVD-coated Titanium Components. Key Eng. Mater., Vols. 348-349: 313-6, 2007.

[25] Y. L. Su, S. H. Yao, C. S. Wei, C. T. Wu, W. H. Kao. Evaluation on the wear, tension and fatigue behavior of various PVD coated materials. Mater. Lett. 35: 255-60, 1998.

[26] Lafer website, www.lafer.eu, (2014).

[27] S. Baragetti, R. Gerosa, F. Villa. WC/C coating protection effects on 7075-T6 fatigue strength in an aggressive environment, in XVII International Colloquium on Mechanical Fatigue of Metals. Procedia Eng. 74:33-6, 2014.

[28] S. Baragetti, R. Gerosa, F. Villa. Fatigue behaviour of thin coated Al 7075 alloy with low temperature PVD coatings. Key Eng. Mater. 577-578: 221-4, 2014.

[29] International Organization for Standardization. ISO 1143 Standard: Metallic materials – Rotating bar bending fatigue testing, 1975.

[30] R. L. Johnston, R. E. Johnson, M. Glenn, W. L. Castner. Stress-Corrosion Cracking of Ti-6Al-4V in methanol. NASA, Washington, D. C., 1967.

[31] R. Johnson. Nasa Experiences with Ti-6Al-4V in methanol. DMIC Memorandum 228, Battelle Memorial Institute, Columbus, 1967.

[32] S. Baragetti. Corrosion fatigue behaviour of Ti-6Al-4V in methanol environment. Surf. Interface Anal. 45: 1654-8, 2013.

[33] S. Baragetti. Notch Corrosion Fatigue Behavior of Ti-6Al-4V. Materials 7: 4349-66, 2014.

[34] D. C. Maxwell, T. Nicholas. A Rapid Method for Generation of a Haigh Diagram for High Cycle Fatigue. Fatigue and Fracture Mechanics: 29th Volume, ASTM, 1999.

[35] T. Nicholas. Step loading for very high cycle fatigue. Fatigue Fract. Eng. Mater. Struct. 25: 861-9, 2002.

[36] R. S. Bellows, S. Muju, T. Nicholas. Validation of the step test method for generating Haigh diagrams for Ti–6Al–4V. Int. J. Fatigue 21: 687-97, 1999.

8. List of figure headings and size

(1 column)

Fig. 1 Typical behavior of PVD coated steel substrates: (a) non-crossing positive contribution of the coating [19,20]; (b) cross-over at $1 \cdot 10^5$ cycles, with beneficial contribution of the PVD coating at higher fatigue lives caused by residual stresses and detrimental contribution for lower fatigue lives due to excessive coating deformations at high applied stresses [21,25].

(1 column)

Fig. 2 Hourglass rotating bending fatigue geometry, according to the ISO 1143 standard [29].

(2 columns)

Fig. 3 Rotating bending step loading fatigue tests results in terms of fatigue strength for $N = 2 \cdot 10^5$ cycles on 7075-T6 uncoated and WC/C coated specimens, in laboratory air and in reagent grade methanol environment: (a) fatigue strength limits for rough surface preparation with 1200 grit paper; (b) fatigue strength limits for mirror-like polished specimens.

(2 columns)

Fig. 4 WC/C coated specimens tested in air with different finishing: pictures (a) and (b) refer to the diamond polished sample tested at 208 MPa – (b) is a magnification of (a) in the crack nucleation zone; pictures (c) and (d) refer to the 1200 grit paper polished sample tested at 234 MPa – (d) is a magnification of (c) in the crack nucleation zone.

(2 columns)

Fig 5 WC/C coated specimens tested in methanol solution with different finishing: pictures (a) and (b) refer to diamond polished sample tested at 189 MPa – (b) is a magnification of (a) in the crack nucleation zone; pictures (c) and (d) refer to 1200 grit paper polished sample tested at 155 MPa – (d) is a magnification of (c) in the crack nucleation zone.

(1 column)

Figure 6. Uncoated diamond polished specimen tested in methanol solution at 195 MPa.

9. Tables

Table 1. Chemical composition of the tested 7075-T6 aluminum alloy

Al [%]	Zn [%]	Mg [%]	Cu [%]	Fe [%]	Si [%]	Cr [%]	Mn [%]	Ti [%]
Bal.	5,6	2,55	1,75	0,32	0,25	0,22	0,2	0,12

Table 2. Confirmation run failure number of cycles N_{conf} obtained for the $2 \cdot 10^5$ fatigue strengths for different samples

Specimens	Environment	$S_{N = 2 \cdot 10^5}$ [MPa]	N_{conf}
Uncoated, as polished	Air	274	$1.2 \cdot 10^5$
Uncoated, as polished	Methanol	195	$2.5 \cdot 10^6$
Uncoated, 1200 grit paper	Air	238	$4.5 \cdot 10^5$
WC/C coated, 1200 grit paper	Air	234	$3.0 \cdot 10^5$
WC/C coated, as polished	Methanol	189	$1.2 \cdot 10^6$